# Synthesis of Activated Carbons from Plastic Waste and Elimination of Rhodamine B in Batch Mode

By
A.B. Boukongou, T. Andzi Barh and P.R. Ongoka

ISSN 2319-3077 Online/Electronic
ISSN 0970-4973 Print

Index Copernicus International Value
IC Value of Journal 82.43 Poland, Europe (2016)
Journal Impact Factor: 4.275
Global Impact factor of Journal: 0.876
Scientific Journals Impact Factor: 3.285
InfoBase Impact Factor: 3.66

J. Biol. Chem. Research
Volume 38 (1), 2021 Pages No. 32-43

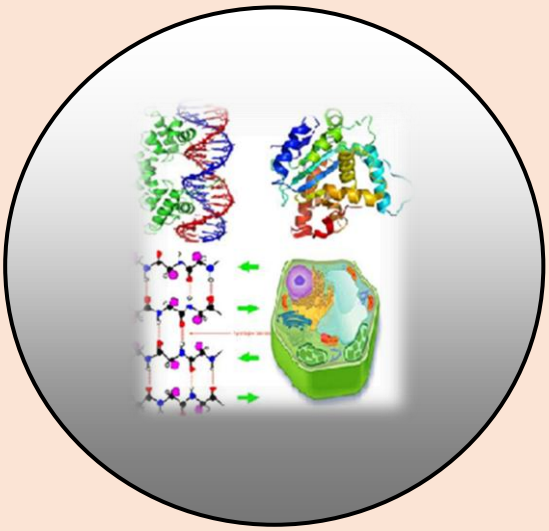

Journal of Biological and Chemical Research

An International Peer Reviewed / Referred Journal of Life Sciences and Chemistry

Indexed, Abstracted and Cited in various International and National Scientific Databases

Published by Society for Advancement of Sciences®

J. Biol. Chem. Research. Vol. 38, No. 1, 32-43, 2021
(An International Peer Reviewed / Refereed Journal of Life Sciences and Chemistry)
Ms 38/01/4080/2021

ISSN 2319-3077 (Online/Electronic)
ISSN 0970-4973 (Print)

T. Andzi Barh
http:// www.sasjournals.com
http:// www.jbcr.co.in
jbiolchemres@gmail.com

RESEARCH PAPER

Received: 13/01/2021 Revised: 12/01/2021 Accepted: 13/01/2021

# Synthesis of Activated Carbons from Plastic Waste and Elimination of Rhodamine B in Batch Mode

**A.B. Boukongou, T. Andzi Barh and P.R. Ongoka**

**Applied Chemistry Research Laboratory, Ecole Normale Superieure (ENS), Marien NGOUABI University, BP: 69, Brazzaville-CONGO**

## ABSTRACT

***In this study, PET waste is used to prepare PETA (a) and PETA (b) activated carbon in "Carbolite Gero CWF-1100, 30-1100 °C" furnace. Zinc chloride was used as impregnating agent. The surface functions were demonstrated using FTIR infrared analyzes. The iodine value of activated carbon obtained by indirect process is higher (1018.32 mg/g) compared to that obtained by direct process (988.56 mg/g). The specific surfaces are respectively 828.326 and 1090.735 $m^2$/g for PETA (a) and PETA (b). The influence of mass has shown that, for 0.01g, the PETA (b) eliminates yield is 62.58 % compared to PETA (a) (45.76 %). pH study shows an increase of RB adsorbed when the pH is between 2 and 4. The ionic strength revealed that RB adsorbed, in the absence of NaCl, are lower than those obtained in the presence of NaCl. Theoretical model of Langmuir show best correlation for two materials, while Freundlich model, described the mechanism of PETA (a). These models suggest that the adsorption of this dye is physico-chemical type. Intraparticle kinetic and Langmuir-Hinshelwood (L-H) models explain the adsorption kinetics on our two materials.***
***Keywords: Activated Carbon, Waste plastic, Adsorption, Rhodamine B and Chemical Kinetic.***

## INTRODUCTION

Environmental pollution problems are becoming more and more important due to the various impacts they could cause such as the extinction of species, damage to the environment and the spread of diseases. This is due to the production of industries responsible for the release of dangerous products in gaseous, liquid and solid forms. But there is also the exponential consumption of products such as plastic, which is trapped in the movement of ocean stream (Chartier Marcel, 1974). However, plastics are not the only pollutant visible in aquatic environments, there is also wastewater, poorly or untreated, containing organic micropollutants, mineral micropollutants and organometallic micropollutants (Rahman et al., 2015). The micropollutants in surface water can disrupt the metabolism of aquatic organisms and modify the structure of the aquatic community. Among these pollutants, there may be mentioned dyes. The latter are discharged into the waters by the textile production units. They are hardly biodegradable (Kifuani et al., 2012, Andzi et al., 2020, Mbaye, 2014, Siragi et al., 2017). The aim of this work is to prepare an activated carbon from waste plastics (Polyethylene Terephthalate), to determine its textural, physical and chemical properties, then to study the adsorption of a prototype organic compound, Rhodamine B (RB). The isotherms models (Langmuir and Freundlich) are used to elucidate the phenomena of absorption.

We use Kinetic models of intra-particle diffusion and Langmuir- Hinshelwood (L-H) to understand the reaction mechanisms at the surface of the carbon synthesized. The adsorption kinetics study describes the rate at which solute is retained on the surface of the adsorbent. This study permits to control the residence time of adsorbate in the interface of solid-solution.

## MATERIALS AND METHODS

### Waste material

Polyethylene terephthalate (PET) plastic waste, commonly called super mont bottles in Cameroon, is collected from urban waste. They are washed, cut into small particles, dried in the sun for 72 hours, and then kept in an oven at 110 °C for 24 hours. After drying, they are used for the preparation of activated carbon.

### Immediate analysis

It consists in determining the characteristics of plastic waste (PET), in particular the ash content, volatile matter, fixed carbon and the humidity level. These analyzes are carried out according to AFNOR XP CEN / TS 14775, XP CEN / TS 14774-3 and XP CEN / TS 15148 standards (Kifuani et al., 2012, Andzi et al., 2020). The experiments are repeated three times to ensure the reproducibility of the results.

### Preparation of activated carbon

The carbonization and activation of plastic waste are carried out in a "Carbolite Gero CWF-1100, 30-1100 ° C" type chamber reactor. Two methods were used.

- The direct process consisted of impregnating the PET waste with $ZnCl_2$. The samples are dried in an oven at 110 °C. The whole set is then heated in an oven at 700 °C at a heating rate of 10 °C/min to obtain the activated carbon PETA (a).
- By the indirect process, the carbonisate is impregnated with Zinc chloride, then oven dried at 110 °C. The whole set is heated in an oven at 700 °C with a heating rate of 10 °C/min in order to obtain the PETA (b).

### Physicochemical characterization of materials

The iodine Index (IN) and methylene blue Index (IBM) were determined to obtain information on the activation degree and the absorption surfaces available in micro and mesopores. The specific surface area was determined using the methylene blue adsorption method (MBAM) (Kifuani et al., 2012, Andzi et al., 2020). The surface chemistry has been elucidated by Fourier Transform Infra-Red Spectroscopy (FT-IR).

### Adsorption of Rhodamine B

The adsorption tests were carried out in a batch reactor by shaking the solutions of Rhodamine B in the presence of the adsorbents. Then, we studied the effect of mass adsorbent, pH of medium, time contact and initial concentration of the dye. The mass varied from 0.01 to 0.05 g, the pH from 2 to 12, the contact time from 5 to 60 min and the initial concentration ranging from 7, 10, 12, 15 and 20 ppm. The amount active carbon is set at 0.01g in 20 mL of RB solution. The effect of ionic form was also studied by varying the content of NaCl from: 0.1, 0.2, 0, 3, 0.4 and 0.5M. The concentration of Rhodamine B is set at 20 ppm (*Andzi et al., 2020)*. The influence of temperature on the adsorption capacity of our activated carbons has been studied for temperatures ranging from 25 °C to 50 °C with gradients of 5 °C. The residual concentration of dyes is determined using a UV-visible spectrophotometer from *LOVIBOND.* The absorbance measurement was performed after centrifugation using a multipurpose flask shaker TT12F. Equation (1) allowed the determination of the amount of dye adsorbed at equilibrium and t time.

$$q_e = \frac{(C_0 - C_e).V}{m} \quad (1)$$

### Modeling of Rhodamine B adsorption isotherms

The theories of adsorption mechanisms on materials are studied with the modeling of adsorption isotherms. This study makes use of the Langmuir and Freundlich models for liquid adsorption (Andzi et al., 2020).

### Kinetic surface reaction models

Rhodamine B adsorption kinetics were performed to determine the adsorbent-RB contact time necessary to reach adsorption equilibrium. This discoloration kinetics was carried out from 0 to 60 minutes, with a gradient of 10 minutes, at room temperature (26 ± 1°C). Kinetic models of intra-particle diffusion and the Langmuir-Hinshelwood model (L-H) were used (Andzi et al., 2020).

## RESULTS AND DISCUSSION

### Immediate analysis

**Table 1. Results of the immediate analysis.**

| Materials | C (%) | W (%) | MV (%) | CF (%) |
|---|---|---|---|---|
| **PET** | 0,013 ± 0,006 | 0,019 ± 0,002 | 95,700 ± 0,020 | 04,268 ± 0,009 |

C (%): Ash, W (%): humidity, MV (%): Volatile Matter, CF (%): Fixed Carbon

The very low ash content of the PET (0.013 %) indicates a very large organic matrix and the absence of inorganic oxides. The absence of uncarbonized compounds and the high carbon content in these samples indicate good carbonization of the precursor material**.** The material prepared therefore constitute essentially of carbon. The high volatile content (95.7 %) of PET waste suggests that activated carbons prepared from this material will have: a good degree of graphitization, a very higher calorific value and a large amount of functional groups (Mbaye, 2014, Iaq et al., 2017). Table 1 also reveals a very low moisture content (0.019 %) of PET. These results suggest that PET waste is compatible for the preparation of activated carbon. However, the high volatile matter content of the plastic precursor could affect the synthesis yield.

### Physicochemical characterization of Active Carbon

### Iodine and Methylene Blue Index

**Table 2. Iodine (IN) and Methylene Blue (IBM) Index.**

| Active Carbon | PETA(a) | PETA(b) |
|---|---|---|
| IN (mg/g) | 988,56 | 1018,32 |
| IBM (mg/g) | 367,43 | 407,34 |

The results of iodine adsorption allow verifying the effectiveness and importance of activated carbons for the elimination of small molecules, in particular dyes and ions, in aqueous solutions. Indeed, the results of this study show that the iodine index (IN) of activated carbons vary from 988.56 to 1018.32 mg/g. We can observe a strong improvement in the microporosity of the materials obtained by indirect process (b) compared to those obtained by direct process (a). This can be explained by the interactions of electrical moments of the porogenic agent ($Zncl_2$) with the oxygen functions which can produce clusters that block the passage of iodine or small molecules to the micropores. On the other side, indirect process (b) suggests a good reactivity of the porogenic agent with the carbonizate. Otherwise, adsorption of methylene blue (IBM) allows verifying the effectiveness and importance of activated carbons for the elimination of large molecules in aqueous solutions. The methylene blue index vary from 367.43 to 407.34 mg/g, either a gap of 39.91 mg/g in mesoporosity. This indicates the presence of super micropores and mesopores. These results reveal that the type of activating agent influences, very significantly, porosity of actived carbons. It develops an affinity between active carbons and methylene blue and suggests the presence of a mesopores and/or macropores structure. This latter, generally serve as the gateway to mesopores (Rahman et al., 2015, Andzi et al., 2020).

### Identification of surface functions by FT-IR

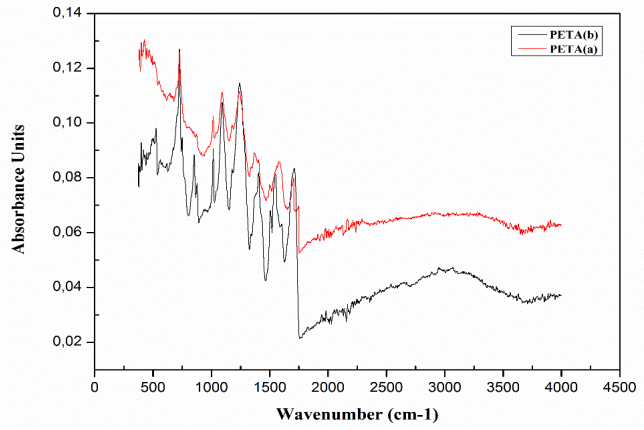


**Figure 1. FTIR spectrum of activated carbon PETA (a) and PETA (b).**

**Table 3. Bands and chemical functions on the surface of PETA (a).**

| Wave number ($cm^{-1}$) | Intensity | Attributions |
|---|---|---|
| 727,225 (600-800) | strong | C-Cl elongation |
| 869,82 (840-790) | | Deformation out of plane (=CH) |
| 1013 (1050-1000) | | -CO, Esther's -CH2-O-C,elongation |
| 1165,64 (1200-1125) | | C-O, Tertiary alcohol, elongation |
| 3387 (3200-2500) | low | OH, LH intermolecular chelated, elongation |

**Table 4. Bands and chemical functions on the surface of PETA (b).**

| Wave number($cm^{-1}$) | Intensity | Attributions |
|---|---|---|
| 727,225 (600-800) | strong | C-Cl elongation |
| 853,84 (840-790) | | Deformation out of plane (=CH) |
| 1093,13 (1300-1050) | | -CO, δ-lactones and larger cycles, elongation |
| 1242,51 (1350-1260) | | OH, secondary alcohol, deformation in the plane |
| 1404 (1410-1310) | | O-H deformation in the plane |
| 1545,97 (1580-1490) | low | N-H deformation in the plane |
| 1710,3 (1715-1690) | strong | C=O (Acid) elongation, dimer (aliphatic) |

Infrared spectroscopy analysis allows identifying the main chemical functions on the surface of our activated carbon. Figure 2 shows the spectra obtained, Table 3 and 4 groups together chemical functions identified. The low absorption band of 3200-2500 $cm^{-1}$ corresponds to the vibrations of hydrogen elongation of hydroxyl groups O-H (H-intramolecular bond chelate). TFIR spectra show absorption bands between 2930 and 2850 $cm^{-1}$ mainly resulting from elongation vibration C–H of aliphatic molecules: carboxyl, phenols or alcohols and chemisorbed water (Vijayakumar et al., 2012). Between 1200-1125 $cm^{-1}$, CO stretching vibration of tertiary alcohols (Vijayakumar et al., 2012, Essomba et al., 2014, Gouli et al., 2008, Myers et al., 1965) .The strong absorption band of 1300-1050 $cm^{-1}$ corresponds to the elongation vibrations of the CO groups of δ-lactones and larger cycles. The small band around 1700 $cm^{-1}$ is attributed to the elongation vibrations of the C=O groups of ketones, aldehydes, lactones or carboxyl. It also appears on the spectrum a band between 3000-3100 $cm^{-1}$, due to the elongation vibrations of the aromatic $C_{tri}$-H bonds. The bands between 1000 and 1350 $cm^{-1}$ are assigned to the vibrations of the C-O bonds and between 2260-2190 $cm^{-1}$ to the vibrations of the acetylene bonds. The band at 1587 $cm^{-1}$ corresponds to the extension vibration of the C=C bond of aromatic compounds. The band at 1166 $cm^{-1}$ corresponds to the C-O vibration of the ether oxide groups. The band at 889 $cm^{-1}$ corresponds to the vibration of meta-substituted benzene and the band at 472 $cm^{-1}$ to the vibration O-Zn. We can see that $ZnCl_2$ impregnation promotes the formation of carboxylic acid groups than lactone or phenol acid functions. The high proportion of surface acid functions gives the activated carbons PETA (b), a high polarity and hydrophilicity and increases negative charge density in the surface (Kifuani et al., 2012, Siragi et al., 2017). Some authors (Myers et al., 1965, Djilani et al., 2012, Byrne et al., 1997) believe that one of the intermediate compounds is the levoglucosan. Its formation takes place between 200 and 400 °C and it is indicated by the carbonyl vibration band (C = O) around 1700 $cm^{-1}$. On our IR spectra, this band is visible for PETA (b).

**Table 5. Specific Surfaces of Synthesized Activated Carbon.**

| Active Carbon | $Q_{mL}$ (mg/g) | $Q_{mL}$ (mol/g) | $S_{BM}$ ($m^2$/g) | R ($l.mol^{-1}$) |
|---|---|---|---|---|
| PETA(a) | 250,000 | 0,000786 | 828,326 | 0,99621 |
| PETA(b) | 331,126 | 0,001035 | 1090,735 | 0,99738 |

Table 5 indicates a variation in the specific surface of 828.326 to 1090.735 $m^2$/g. It emerges that the activated carbon PETA (b) has a higher specific surface than PETA (a). Activation temperature (700 °C), impregnation ratio, reaction time and slow heating rate (10 °C/min) have effects on the porosity. It can be observed that the carbonizate impregnation presents good reactivity between $ZnCl_2$ and carbon matrix, which has favored the enlargement of the existing pore volumes and the formation of new pores.

**Determination of the specific surface**

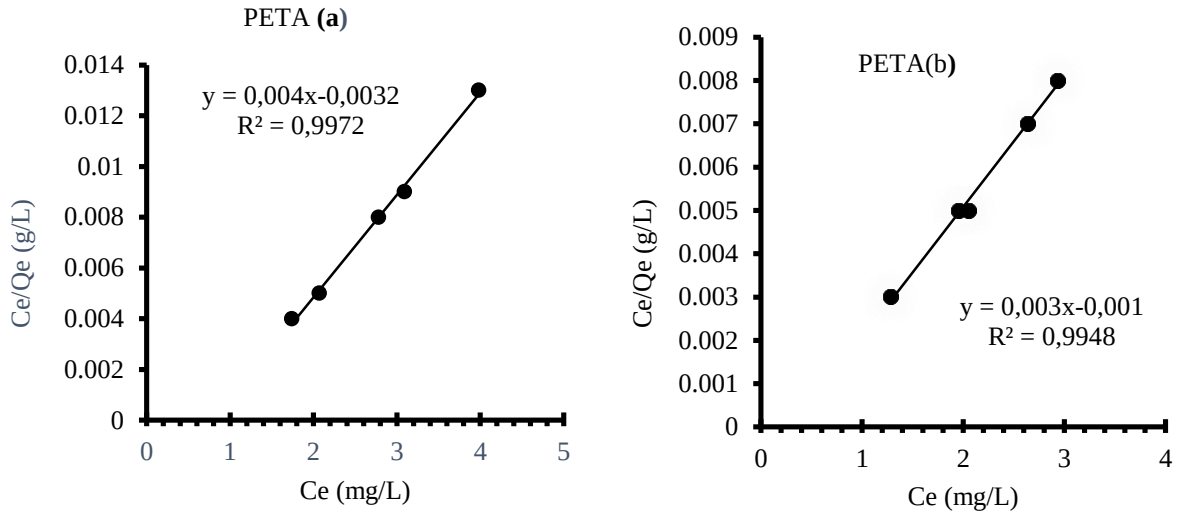


**Figure 2. Langmuir isotherm of BM for PETA (a) and PETA (b).**

**Study of adsorption equilibrium of Rhodamine B in aqueous solution**
**Effect of stirring time**

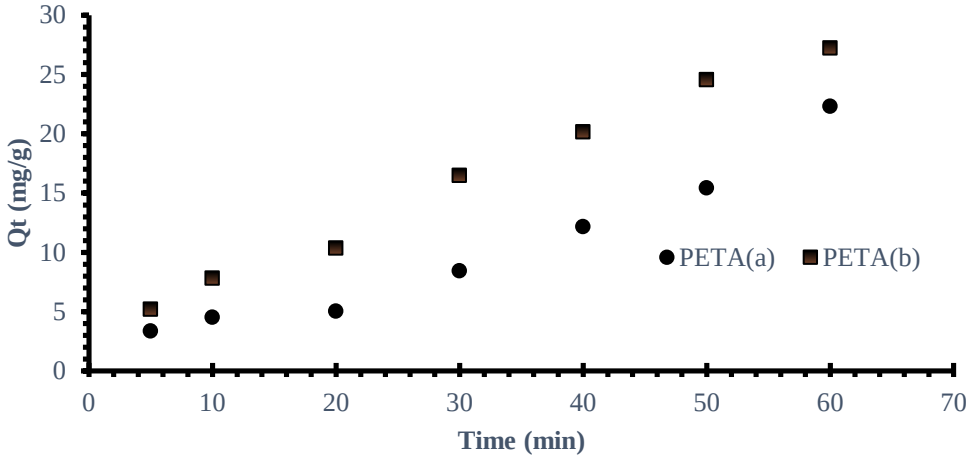


**Figure 3. Quantity of RB adsorbed as a function of stirring time.**

Figure 3 shows the efficiency of our activated carbons over time, during the adsorption of Rhodamine B. The evolution of the adsorbed amounts of Rhodamine B (mg/g), as a function of time, shows a slight progression the first 20 minutes and gradual growth after 40 minutes for PETA (a) and 50 minutes for PETA (b). There is also an attenuated increase until equilibrium is reached after sixty (60) minutes for all materials. Moreover, the extension of this time does not lead to a significant improvement in the percentage of disappearance of this compound.

These observations are explained by the fact that during the first minutes there is a maximum availability of active sites on the surface of the adsorbents. As soon as Rhodamine B binds to the adsorbent, there is a slowing down of the adsorption rate. Because, the pores of these begin to be saturated, preventing the attachment of other molecules (Andzi et al., 2020).

**Effects of initial concentration**

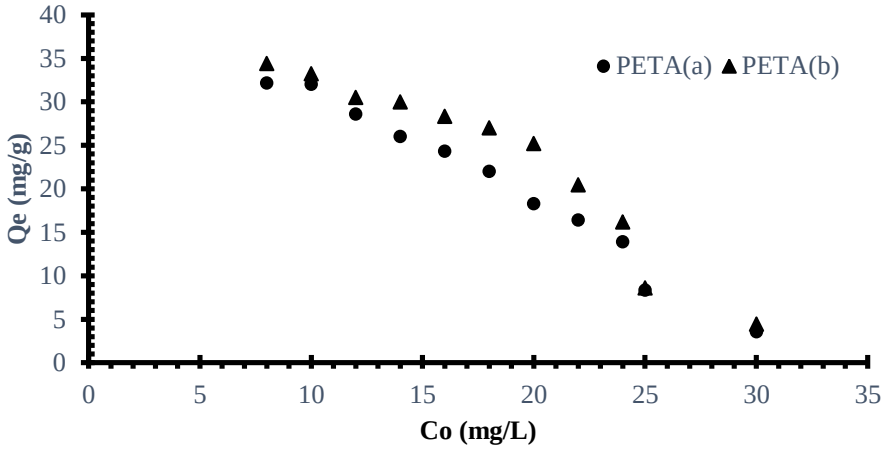


**Figure 4. Quantity of RB adsorbed as a function of the initial concentration.**

Figure 4 show that the amount of Rhodamine B adsorbed decreases with increasing concentration. This may be due to the agglomeration/aggregation of adsorbent particles at higher masses. This situation limits the surface area available for adsorbents and increases the length of the diffusion path (Tang et Bacon, 1964, Bikales et Segal, 1971). Thus we can notice that our activated carbon absorbs high amounts of RB at low concentrations.

These elimination characteristics indicate that the saturation of mesopore depends on the initial concentration. Rhodamine B binds to active sites at a concentration of less than 12 mg/L. The strong adsorption at the initial concentration may be due to a greater number of empty sites available on the adsorbents at the initial stage. The amount of Rhodamine B adsorbed decreases with increasing initial concentration, due to the accumulation of RB particles on the surface of activated carbon (Tzong-Horng, 2010).

**Effect of pH**

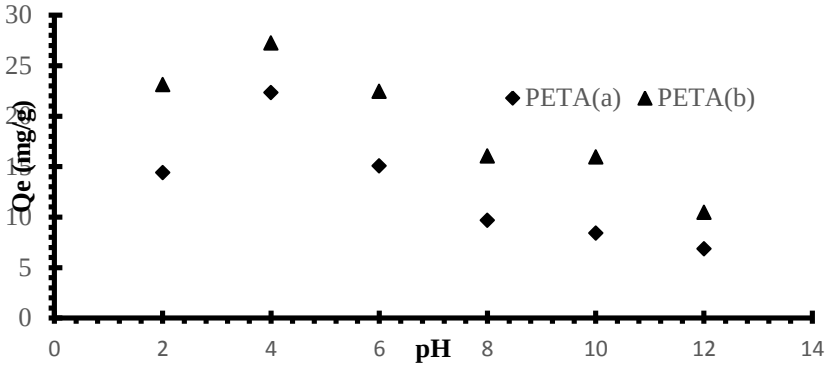


**Figure 5. Quantity of RB adsorbed as a function of pH.**

The pH is an important parameter which influences the adsorption of pollutants, because it affects the surface of the adsorbent and the adsorbate (Kunquan at al., 2009, Jia et Lua, 2008). This study shows an increase in the quantity of RB adsorbed when the pH of the solution is between 2 and 4 (Figure 5).

In this pH range, the molecular form of the dye persists in the solution and the protonation of the surface is minimum, leading to an improvement in the adsorption of RB, which reaches its maximum at pH = 4.

At acidic pH, our adsorbents, being positively charged, all exhibits a deficit in electrons, so there should be repulsion, and therefore a small amount of Rhodamine B adsorbed. The large quantities of RB adsorbed at these pH ($2 \leq pH \leq 4$) could be explained by the fact that it is the electrons of the aromatic nuclei of our electron-rich adsorbents which fill the electronic deficit present on our adsorbents, thus promoting the diffusion of RB on PETA (b) and PETA (a) (Andzi et al., 2020).

**Effect of Mass**

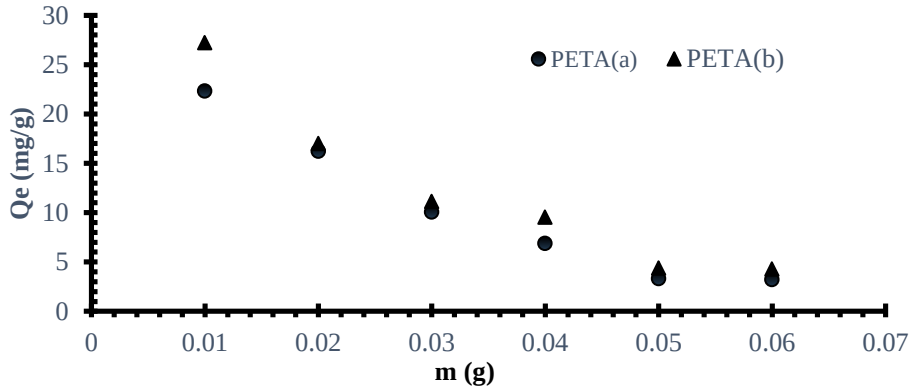


**Figure 6. Quantity of RB adsorbed as a function of mass.**

**Effects of Ionic Strength**

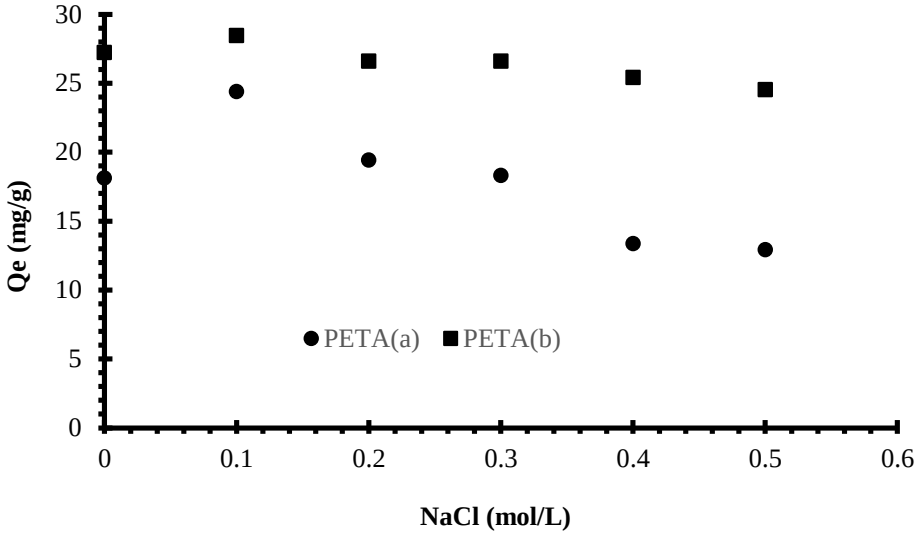


**Figure 7. Amount of RB adsorbed as a function of the NaCl concentration.**

Figure 6 shows a decrease in the adsorbed quantity of the pollutant as a function of the mass of the adsorbent. This amount absorbed is inversely proportional to the increase of adsorbents mass. Beyond 0.05 g, the retention rate decreases slightly, probably indicating the presence of electrostatic interactions, between the molecules of Rhodamine B and the adsorbent materials. This leads to the formation of aggregates due to the agglomeration of these particles on the surface of the adsorbents. There is therefore a reduction in the contact surface, because the active sites of these materials become masked. This situation leads to an increase in the path of diffusion of the pollutant in solution (Jadhav et Vaujara, 2004).

Figure 7 shows that the ionic strength increases when the concentration of NaCl increases. A higher ionic concentration leads to a strong fixation of the RB. This would be due to the partial neutralization of the positive charge on the surface of the activated carbon and to a compression of the electrical double layer by the Cl- anion. The presence of Cl- ions will allow the pairing between negative charges (-) of active carbon and the positive charge (+) of RB, which results in the reduction of the repulsion between the molecules adsorbed to the surface. It is observed that RB adsorbed, in the absence of NaCl, are lower than those obtained in the presence of NaCl. We note concentrations ranging from 18.304 to 27.223 mg/g in the absence of NaCl, against 24.393 to 28.455 mg/g in the presence of NaCl. This result suggests that ionic strength increases the adsorption capacity of RB.

**Effect of Temperature**

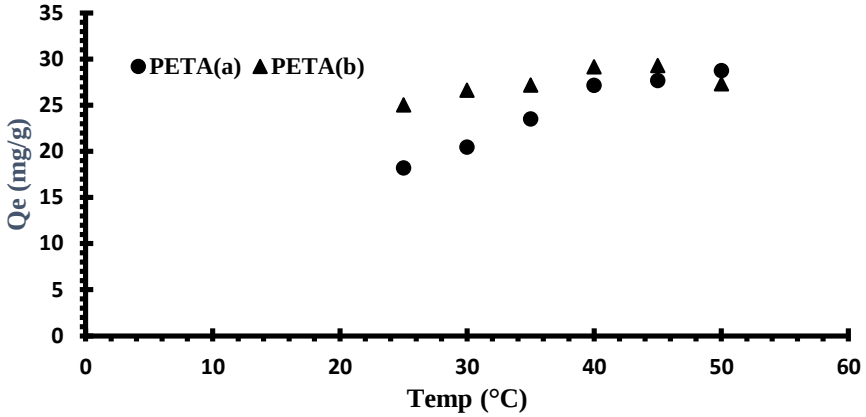


**Figure 8. Effect of Reactor Temperature on RB Adsorption.**

It emerges from this study (Figure 8) that the quantity of the adsorbed dye increases with the temperature gradient of the adsorbate. This is well observed for the two activated carbons, with some differences for PETA (b) on which we observe a decrease in the quantity adsorbed from 45 °C. This result indicates that the adsorption follows an endothermic mechanism which would increase the mobility of the ionized molecules of the dye and would produce an enlargement of the pores in the internal structure of the adsorbent. Therefore, adsorption capacity is expected to largely depend on the chemical interaction between functional groups on the adsorbent surface and adsorbed molecules. This can be explained by an increase in the diffusion rate of adsorbate through the pores, since diffusion is an endothermic process. However, the decrease in the adsorption capacity observed, on PETA (b) activated carbon with temperature, indicates that the process is exothermic from 45 °C, due to the desorption step in the adsorption mechanism. It is known that the decrease in adsorption capacity with increasing temperature is mainly due to the weakening of the adsorptive forces between active sites on the adsorbent, dye molecules and also between dye molecules adjacent to the adsorbed phase. The experimental results prove that this parameter positively affects this process by a strong energy contribution, thus making it possible to overcome the repulsive forces located at the level of the interfaces of liquid and solid medium. So, it is interesting to note that the heating input plays an important role in the retention kinetics of this dye, regardless of their affinity for this support. This means that the retention process could be, on the one hand, endothermic (ΔH > 0) for PETA (a) leading under these conditions to chemisorption and, on the other hand, exothermic for PETA (b).

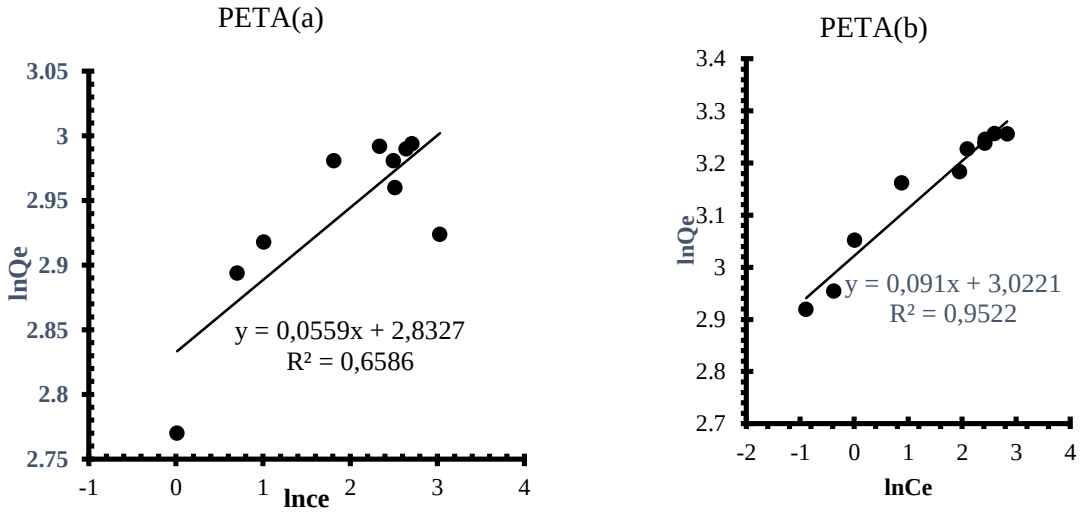


**Figure 9. Freundlich Adsorption Model isotherms of PETA (a) and PETA (b).**

**Modeling of Adsorption Isotherms**

**Freundlich Adsorption Model**

The linear Freundlich transform gives the curves lnQe = f (Ce) represented by figure 9 and the parameters recorded in Table 6.

**Table 6. Freundlich Adsorption Model Parameters.**

| Adsorption Model | Parameters | PETA(a) | PETA(b) |
|---|---|---|---|
| **Freundlich** | r | 0,65862 | 0,99804 |
| | σ | 0,0149 | 0,0098 |
| | $K_F$ (L/g) | 16,992 | 19,94 |
| | 1/n | 0,056 | 0,11205 |

The plot of lnQe = f (lnCe) allows the graphical determination of 1/n and ln Qe respectively slope and y-intercept of the regression line. It is noted (Table 6) that the Freundlich parameters 1/n are 0.056 and 0.612. These values are between 0 and 1, which suggests a physicochemical adsorption process. PETA (b) activated carbon has a high $K_F$ value (19.94 L/g) compared to that of PETA (a) (16.992 L/g). Moreover, the value of the correlation coefficient (r = 0.99804) of PETA (b), shows that Freundlich model describes his adsorption mechanism and the adsorption process take place on a non-homogeneous surface with an interaction between the adsorbed molecules. However, correlation coefficient (r = 0.65862) of PETA (a) is less than 0.95, which means that Freundlich adsorption model does not explain the point of distribution or the absorption mechanism for this activated carbon.

**Langmuir Adsorption Model**

The linear Langmuir transform applied to the two (02) adsorbents allows obtaining Figure 10 and the parameter results reported in Table 7.

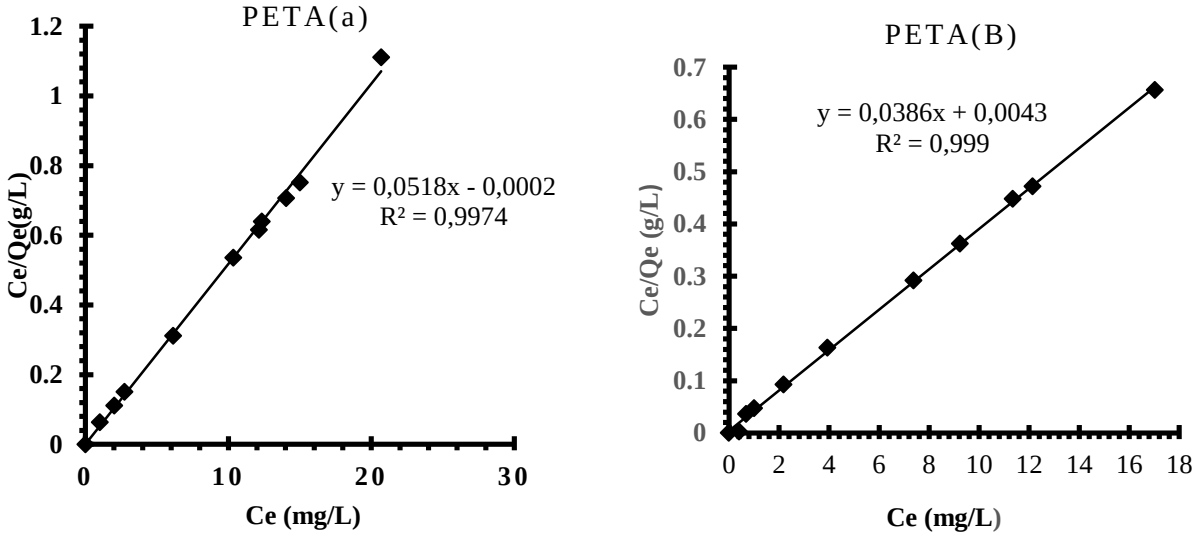


**Figure 10. Langmuir Adsorption model isotherms of PETA (a) and PETA (b).**

**Table 7. Langmuir Adsorption Model Parameters.**

| Adsorption Model | Parameters | PETA(a) | PETA(b) |
|---|---|---|---|
| **Langmuir** | r | 0,99742 | 0,9998 |
| | σ | 0,0091 | 0,0003 |
| | $Q_m$ (mg/g) | 19,321 | 25,906 |
| | $K_L$ (L/mg) | -0,022 | 9,019 |
| | $R_L$ | 0,698 | 0,006 |

The Langmuir constant $K_L$ measures the intensity of adsorption. Indeed, when $K_L$ is large, the affinity is strong between the adsorbent and the adsorbate. The correlation coefficients (r> 0.95) show the adequacy between the Langmuir model and the experimental data, it also appears that, the regression equation is adapted to describe the distribution points and the mechanism reaction of activated carbons PETA (b) and PETA (a). For the PETA (b) sample, a favorable and irreversible adsorption is observed, justified by the Langmuir constant $R_L$ ($0<R_L<1$). It appears that the interactions between the molecules adsorbed on the surface are zero or negligible. Langmuir's model is more suitable for studying the adsorption of RB on the two materials.

**Kinetics Models**

**Intra-particle Diffusion Kinetic Model**

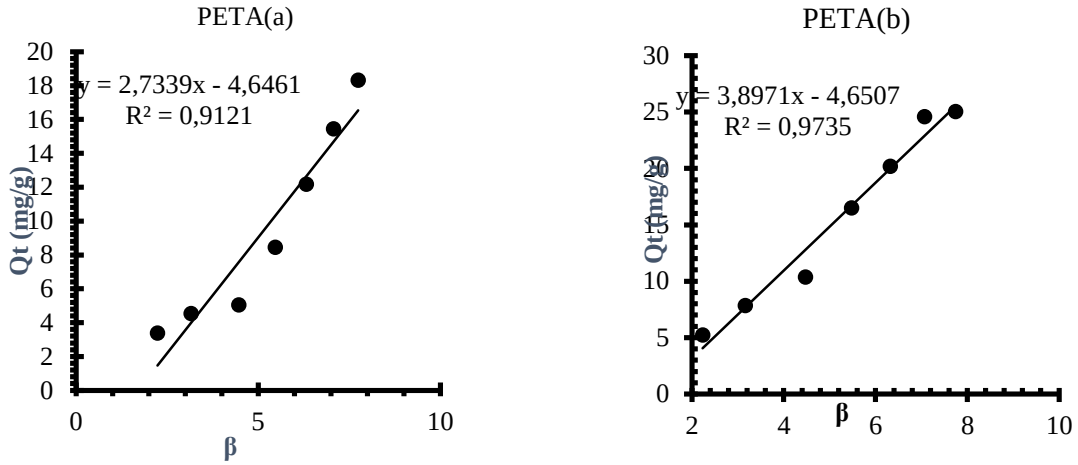


**Figure 11. Intra-particle model of activated carbon PETA (a) and PETA (b).**

**Table 8. Intra-particle model of the adsorption kinetics of Rhodamine B.**

| Kinetic Model | Parameters | PETA(a) | PETA(b) |
|---|---|---|---|
| Intra particle | Kid ($mg.g^{-1}.min^{-1/2}$) | 3,345 | 4,646 |
| | A | 4,087 | 2,734 |
| | r | 0,9832 | 0,9866 |
| | σ | 5,872 | 10,249 |

**The Langmuir-Hinshelwood Kinetic Model (L-H)**

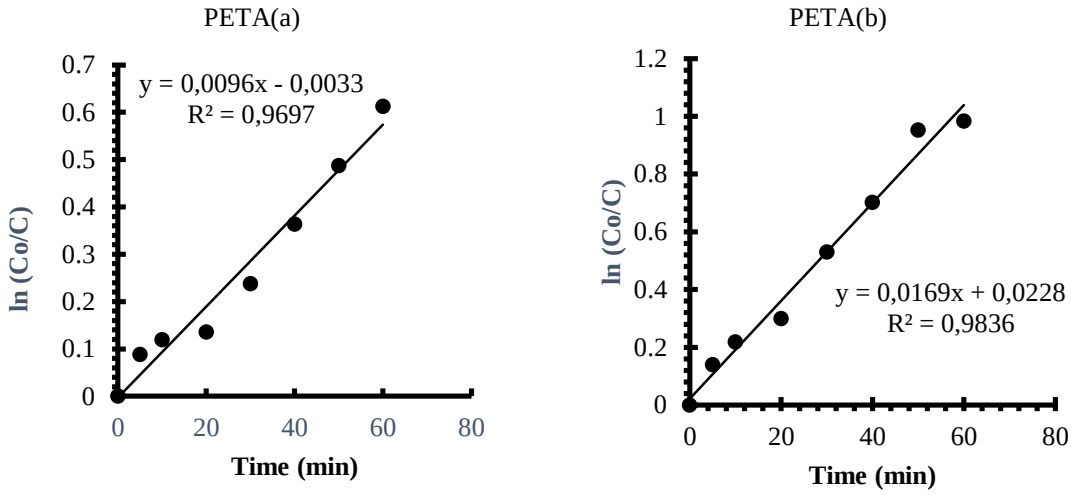


**Figure 12. Langmuir-Hinshwood (L-H) model of Rhodamine B adsorption.**

Figure 11 presents the plots of this model for the active materials studied. The values of the external diffusion constant $k_{id}$ and the correlation coefficients (r) are given in Table 8. From this figure, it can be observed that the correlation coefficients of the 2 materials are greater than 0.95. The values of the constant ($k_{id}$) defining the rate factor of PETA (a) is near that of PETA (b). This assumes that the adsorption process takes place at substantially similar diffusion rates and the process describing adsorption on PETA (b) is relatively different. This difference can be generated by the presence of the δ-lactone groups identified on the surface of PETA (b). This shows that intra particle diffusion is an important step in the process of adsorption of Rhodamine B on the various supports. We can also observe that no regression line goes through the origin. This result therefore suggests that the adsorption of Rhodamine B involves intra particle diffusion. But, this step is not the only factor controlling the rate of adsorption (Andzi et al., 2020). The diffusion constant values imply that the diffusion rate of activated carbon is relatively slow. This promotes the strong interaction between the adsorbents and the adsorbate.

**Table 9. Langmuir-Hinshwood Kinetic Model (L-H).**

| Kinetic Model | Parameters | PETA(a) | PETA(b) |
|---|---|---|---|
| **L-H** | $k'$ | -0,003 | 0,02279 |
| | r | 0,98472 | 0,98084 |
| | σ | 0,00968 | 0,01601 |

We can observe that the correlation coefficients (r) for the kinetic model of Langmuir- Hinshelwood (L-H) are very close to unity (r > 0.95). These results show that the model is applicable on the different activated carbons used. The apparent rate constant k' varies from PETA (a) to PETA (b). k'> 0 describe the competition (RB-$H_2O$) predominated by the molecules of Rhodamine B, such is the case of PETA (b), then k' < 0, show a competition predominated by the molecules of the solvent ($H_2O$), in the case of PETA (a). This can be explained by the fact that our activated carbons develop more affinity for poorly soluble molecules in water (this reduces the adsorption competition between the solvent and the molecule) unlike more soluble molecules such as Rhodamine B (~50 gL-1). It is important to recall that the solvent effect concerns interactions of an electrostatic nature between the acidic carboxylic functions located on the active carbon and the water molecules, thus forming hydrogen bonds. These results suppose that the water molecules are also adsorbed and some sites are no accessible to the dye molecules. This approach could justify the low adsorption capacity of PETA (a).

## CONCLUSION

Two activation processes were demonstrated: the direct activation process, which consisted of impregnating the plastic waste with Zinc chloride ($ZnCl_2$) to obtain PETA (a) and the indirect activation process, which consisted in impregnating the carbonizate with the same impregnating agent, before bringing it to the oven in order to obtain the activated carbon PETA (b). The iodine value of these active carbons prepared by indirect chemical activation is higher (1018.32 mg/g) than that obtained by direct process (988.56 mg/g). The specific surfaces are 828.326 and 1090.735 $m^2/g$ for the PETA (a) and PETA (b) respectively. The hydroxyl, carboxylic and δ-lactone functions were demonstrated at the surface of all the samples using Fourier Transformer Infra-Red (FTIR) analyzes. The influence of the mass on the retention of Rhodamine B has shown that, for a mass of 0.01g, the PETA (b) eliminates a large amount of the pollutant (62.58 %) compared to PETA (a) (45.76 %). There is also an attenuated increase until equilibrium is reached after sixty (60) minutes for all materials. Moreover, extending this time does not lead to a significant improvement in the percentage of disappearance of this compound. The study of the variation in pH shows an increase in the amount of RB adsorbed when the pH of the solution is between 2 and 4. Under this pH range, the molecular form of the dye persists in the medium and the surface protonation is minimal, leading to an improvement in the adsorption of RB, which reaches its maximum at pH = 4. The study of the ionic strength revealed that the quantities of RB adsorbed, in the absence of NaCl, are lower than those obtained in the presence of NaCl. Our experimental results on the adsorption of Rhodamine B were compared with the theoretical models of Langmuir and Freundlich. The best correlation for the two materials was obtained with the Langmuir model, while the Freundlich models, described that the mechanism of PETA (a). These models suggest that the adsorption of this dye on the various carbons is of the physicochemical type. The kinetic intraparticle diffusion model and Langmuir-Hinshelwood (L-H) are applicable to both activated carbons and explain well the reaction mechanisms of adsorption on these materials.

## REFERENCES


**Chartier Marcel, M. (1974).** Les types de pollutions de l'eau. *Norois*, 82, 183-193.

**Rahman, A., Bacaoui, A., Nongwe, I.B. and Ketcha J.M. (2015).** Composite activated carbon from plastic waste and lignocellulosic waste materials, *International Research Journal of Natural and Applied Sciences*, 2, 2349-4077.

**Kifuani Philippe Noki and Mukana V.D. (2012)**. Adsorption de la quinine bichlorhydrate sur un charbon actif peu coûteux à base de la Bagasse de canne à sucre imprégnée de l'acide phosphorique, *Int. J. Biol. Chem. Sci.* 6(3), 1337-1359.

**Andzi Barhé, T., Boukongou, A.B., Ngoma, L.S. and Ongoka, P.R. (2020).** Characterization of activated carbon prepared from lignocellulosic Materials and Kinetic Study of the adsorption of Rhodamine B, *JCBPS*, 10(4), 01-018.

**Mbaye, G. (2014).** Développement de charbon actif à partir de biomasse lignocellulosique pour des applications dans le traitement de l'eau. Thèse de doctorat en technologie de l'Eau, de l'Energie et de l'Environnement. 2iE, Burkina Faso, pp. 215.

**Siragi, D.B., Maazou, H.I. Hima, M.M.M., Alma, Z.A. and Ibrahim, N. (2017)** Elimination du chrome par du charbon actif élaboré et caractérisé à partir de la coque du noyau de Balanites Aegyptiaca. *Int. J. Biol. Chem. Sci.* 11(6), 3050-3065.

**Iaq, N.B., Beenish, M., Muhammad, A.H. and Raziya, N. (2007)**. Removal of Zn (II) ions from aqueous solution using *Moringa oleifera* Lam (Heroseradish tree) biomass, *Process biochemestry*, 42, 547-553.

**Vijayakumar, G., Tamilarasan, R. and Dharmendirakumar (2012).** M. Adsorption, Kinetic, Equilibrium and Thermodynamic studies on the removal of basic dye Rhodamine-B from aqueous solution by the use of natural adsorbent perlite, *J. Mat. Envir. Sci.* 3(1), 157-170.

**Essomba, J.S., Ndi Nsami J., Belibi Belibi, P. D., Tagne G. M. and Ketcha Mbadcam, J. (2014).** Adsorption of cadmium(II) ions from aqueous solution onto kaolinite and metakaolinite. *Pure and Applied Chemical Sciences*, 2 (11), 11- 30.

**Gouli, B.M.I., Yapo, A.J., Ello, A.S., Diabate, D. and Trokourey A. (2008).** Adsorption of acetic and benzoïc acids from aqueous solutions on activated carbon. *Journal de la Société Ouest-Africaine de Chimie*, 026, 53-57**.**

**Myers, A.L. and Prausnitz J.M. (1965).** Thermodynamics of Mixed-gas Adsorption, *AlChE J.,* 11(1), 121-127.

**Djilani, C., Zaghdoudi, R., Modarressi, A., Rogalski, M. and Djazi, F. (2012).** Elimination of organic micropollutants by adsorption on activated carbon prepared from agricultural waste. *Chem. Engin. J.* 189-190, 203-212.

**Byrne, C.E. and Nagle, D.C. (1997).** Carbonization of wood for advanced materials applications. *Carbon*, 35(2), 259–266.

**Tang, M.M. and Bacon, B. (1964).** Carbonization of cellulose fibers—I. Low temperature pyrolysis, *Carbon*, 2(3), 211-214. 1964.

**Bikales, N.H. and Segal**, **L. (1971).** Cellulose and Cellulose Derivatives, Ed. Wiley- Inter Science, New York, p. 381.

**Tzong-Horng, L. (2010).** Development of mesoporous structure and high adsorption capacity of biomass-based activated carbon by phosphoric acid and zinc chloride activation. *Chem. Eng. J.* 158, 129.

**Kunquan, L., Zheng, Z., Xingfa, H., Guohua, Z., Jingwei, F. and Jibiao Z. (2009)** Equilibrium, kinetic and thermodynamic studies on the adsorption of 2-nitroaniline onto activated carbon prepared from cotton stalk fiber. *Journal of Hazardous Materials*. 166, 213-220.

**Jia Q. and Lua A.C. (2008).** Effects of pyrolysis conditions on the physical characteristics of oil-palmshell activated carbons used in aqueous phase phenol adsorption, *J. Anal. Appl. Pyrolysis* 83, 175-179.

**Jadhav, A.N. and Vaujara A.K. (2004).** Removal of phenol from waster using sawdust, polymerized sawdust and sawdust carbon. *Indian Journal of Chemical technology*, 11, 35-41.



**Corresponding author: Dr. T. Andzi Barhé, Applied Chemistry Research Laboratory, Ecole Normale Superieure (ENS) Marien NGOUABI University, BP: 69, Brazzaville-CONGO**
**Email: andzibarhe@gmail.com Tel. +242. 06 624 40 08**